

Controlled Polymerization of Methacrylates to High Molecular Weight Polymers Using Oxidatively Activated Group Transfer Polymerization Initiators

Yuetao Zhang and Eugene Y.-X. Chen*

Department of Chemistry, Colorado State University, Fort Collins, Colorado 80523-1872

Received September 6, 2007; Revised Manuscript Received October 28, 2007

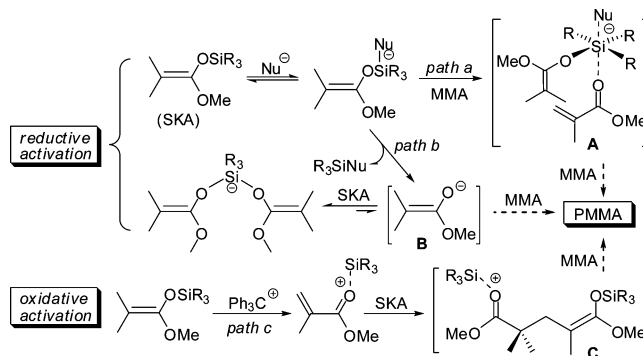
ABSTRACT: Oxidative activation of group transfer polymerization initiator silyl ketene acetals with a catalytic amount of the olefin polymerization activator $\text{Ph}_3\text{CB}(\text{C}_6\text{F}_5)_4$ directly affords the first methyl methacrylate addition product, the highly active propagating species that contains both the nucleophilic and electrophilic catalyst sites to promote the controlled methacrylate polymerization via cooperative catalysis.

Introduction

Polymerization of acrylic monomers such as methyl methacrylate (MMA) by a silyl ketene acetal (SKA) and a nucleophilic or Lewis acid catalyst was termed group transfer polymerization (GTP);¹ this was named such based on the initially postulated *associative* propagation mechanism in which the silyl group remains attached to the same polymer chain and is simply transferred intramolecularly to the incoming monomer through hypervalent anionic silicon species (path a, Scheme 1).¹ However, it has been recently concluded² that several lines of key experimental evidence now support a *dissociative* mechanism,³ which involves ester enolate anions as propagating species and a rapid, reversible complexation (termination) of small concentrations of enolate anions with SKA or its polymer homologue (path b). GTP can readily produce poly(methyl methacrylate) (PMMA) with a number-average molecular weight (M_n) of $\leq 20\,000$ in a controlled fashion at $T \geq$ ambient temperatures, but its synthesis of PMMA in the 60 000 range is difficult.² We reasoned that a combination of a SKA with a silyl cation " R_3Si^+ ", which can be either added externally or generated internally via direct oxidative activation of SKA (vide infra), could promote cooperative catalysis involving a *bimolecular, activated monomer* propagation (path c), thus potentially affording PMMA of a low to high M_n on demand. From a propagation mechanism point of view, path c closely resembles that by the isoelectronic enolaluminate/alane pair⁴ or the zirconocene enolate/zirconocenium pair.⁵

Activation of the inactive SKA or monomer is the critical first step in all the mechanisms shown above. It can be viewed that paths a and b involve *reductive activation* of SKA, whereas path c represents *oxidative activation* of SKA using a trityl salt. Trityl salts are known to catalyze aldol condensations and Michael reactions involving nucleophiles such as silyl enol ethers or SKA and substrates such as acetals, aldehydes, or α,β -unsaturated ketones;⁶ the trityl catalyst used in these reactions was proposed to activate the substrate via interaction between the trityl cation and alkoxy (or acyloxy) or carbonyl oxygen of the substrate.⁶ Trityl tetrakis(pentafluorophenyl)borate (TTPB), $\text{Ph}_3\text{CB}(\text{C}_6\text{F}_5)_4$,⁷ is an important activator for metal-catalyzed olefin polymerization.⁸ Trimethylsilyl triflate catalyzes aldol condensations of enol silyl ethers and acetals,⁹ while the

Scheme 1. Associative, Dissociative, and Bimolecular Pathways for the Methyl Methacrylate (MMA) Polymerization Using a Silyl Ketene Acetal (SKA)



combination of R_3SiOTf with $\text{B}(\text{C}_6\text{F}_5)_3$ mediates efficient GTP of acrylates initiated by SKA.¹⁰

In this contribution, we report a new polymerization system based on *oxidative activation* of SKA with the catalyst $\text{Ph}_3\text{CB}(\text{C}_6\text{F}_5)_4$. The four most remarkable features about this new activation/polymerization system include (a) that it directly affords the first MMA addition product, the highly active propagating species C, (b) that it provides dual activation for both SKA and subsequently the monomer, (c) that it produces low to high M_n ($> 10^5$) PMMA with a narrow molecular weight distribution [polydispersity index $\text{PDI} (M_w/M_n) = 1.04\text{--}1.12$] in a controlled fashion at ambient temperature, and (d) that the catalyst loading can be as low as 0.025 mol % (based on the monomer).

Experimental Section

Materials, Reagents, and Methods. All syntheses and manipulations of air- and moisture-sensitive materials were carried out in flamed Schlenk-type glassware on a dual-manifold Schlenk line, on a high-vacuum line (typically from 10^{-5} to 10^{-7} Torr), or in an argon-filled glovebox (typically < 1.0 ppm oxygen). NMR-scale reactions (typically in a 0.02 mmol scale) were conducted in sealed NMR tubes. High performance liquid chromatography (HPLC) grade organic solvents were first sparged extensively with nitrogen during the filling the 20 L solvent reservoir and then dried by passage through activated alumina [for diethyl ether (Et_2O), tetrahydrofuran (THF), and CH_2Cl_2] followed by passage through Q-5 supported copper catalyst (for toluene and hexanes) stainless steel columns. Benzene- d_6 and toluene- d_8 were dried over sodium/

* Corresponding author. E-mail: eychen@lamar.colostate.edu.

potassium alloy and vacuum-distilled or filtered, whereas C_6D_5Br , CD_2Cl_2 , and $CDCl_3$ were dried over activated Davison 4-Å molecular sieves. NMR spectra were recorded on either a Varian Inova 300 (FT 300 MHz, 1H ; 75 MHz, ^{13}C ; 282 MHz, ^{19}F) or a Varian Inova 400 spectrometer. Chemical shifts for 1H and ^{13}C spectra were referenced to internal solvent resonances and are reported as parts per million relative to $SiMe_4$, whereas ^{19}F NMR spectra were referenced to external $CFCl_3$.

MMA (99%) and *n*-butyl methacrylate (BMA; 99%) were purchased from Aldrich Chemical Co. The monomers were first degassed and dried over CaH_2 overnight, followed by vacuum distillation, and final purification of MMA involved titration with neat tri(*n*-octyl)aluminum (Strem Chemicals) to a yellow end point¹¹ followed by distillation under reduced pressure. The purified monomers were stored in brown bottles inside a $-30\text{ }^\circ\text{C}$ glovebox freezer. Butylated hydroxytoluene (BHT-H, 2,6-di-*tert*-butyl-4-methylphenol) was purchased from Aldrich Chemical Co. and recrystallized from hexanes prior to use. Tris(pentafluorophenyl)-borane $B(C_6F_5)_3$ and TTPB were obtained as a research gift from Boulder Scientific Co.; $B(C_6F_5)_3$ was further purified by recrystallization from hexanes at $-30\text{ }^\circ\text{C}$, whereas TTPB was used as received. Methyl trimethylsilyl dimethylketene acetal (^{Me}SKA , 95%), diisopropylamine ($\geq 99\%$), methyl isobutyrate (99%), triethylsilane (99%), and chlorotriethylsilane (99%) were purchased from Aldrich and dried over CaH_2 , followed by vacuum distillation.

Methyl Triethylsilyl Dimethylketene Acetal (^{Et}SKA). Modified literature procedures¹² were used to prepare ^{Et}SKA . In an argon-filled glovebox, a 200 mL Schlenk flask was equipped with a stir bar and charged with 100 mL of THF and 5.00 mL (3.61 g, 35.7 mmol) of diisopropylamine. The flask was sealed with a rubber septum, removed from the glovebox, and interfaced to a Schlenk line. The resulting solution was cooled to $0\text{ }^\circ\text{C}$, and 23.4 mL of *n*-butyllithium (1.6 M in hexane, 37.5 mmol) was added dropwise via a syringe. After being stirred at $0\text{ }^\circ\text{C}$ for 30 min, 4.09 mL of methyl isobutyrate (3.64 g, 35.7 mmol) was added to this solution. The reaction mixture was stirred at $0\text{ }^\circ\text{C}$ for 30 min, after which 11.98 mL (71.4 mmol) of chlorotriethylsilane was added. The mixture was allowed to warm slowly to room temperature and stirred for 3 h at this temperature. All volatiles were removed in vacuum, and hexanes ($\sim 50\text{ mL}$) were added. The resulting precipitates were filtered off under an argon atmosphere; the solvent of the filtrate was removed in vacuo, and the resulting residue was vacuum-distilled ($45\text{--}46\text{ }^\circ\text{C}$, 0.4 Torr) to give 6.15 g (79.8%) of ^{Et}SKA as a colorless liquid. 1H NMR (C_6D_6 , 300 MHz, $23\text{ }^\circ\text{C}$): δ 3.35 (s, 3H, *OMe*), 1.69 (s, 3H, $=CMe$), 1.66 (s, 3H, $=CMe$), 1.02 (t, $J = 7.8\text{ Hz}$, 9H, CH_2CH_3), 0.69 (q, $J = 7.8\text{ Hz}$, 6H, CH_2CH_3).

Variable-Temperature NMR Studies of the Reaction of ^{Me}SKA with TTPB: In Situ Generation of $Ph_2C=C(CH=CH)_2CHCMe_2C(OMe)=O\cdots SiMe_3[B(C_6F_5)_4]$ (1) and Active Species $Me_3SiOC(OMe)=CMeCH_2CMe_2C(OMe)=O\cdots SiMe_3[B(C_6F_5)_4]$ (2). In an argon-filled glovebox, an NMR tube was charged with 3.5 mg (0.02 mmol) of ^{Me}SKA and 0.3 mL of CD_2Cl_2 . This NMR tube was sealed with a rubber septum, removed from the glovebox, and cooled to $-78\text{ }^\circ\text{C}$. A 0.3 mL CD_2Cl_2 solution of TTPB (18.5 mg, 0.02 mmol) was slowly added to this tube via a syringe. This reaction mixture was kept for 1 h at $-78\text{ }^\circ\text{C}$. NMR Spectra were recorded from $-80\text{ }^\circ\text{C}$ to room temperature by $10\text{ }^\circ\text{C}$ intervals after having equilibrated at each temperature for at least 15 min. Compound 1 was formed cleanly at $-80\text{ }^\circ\text{C}$; at temperatures $\geq -70\text{ }^\circ\text{C}$, it began to convert to compound 2 which was obtained cleanly at $-50\text{ }^\circ\text{C}$, but is somewhat unstable at temperatures $\geq -40\text{ }^\circ\text{C}$. The reaction in a 2/1 ^{Me}SKA /TTPB ratio yielded the same species as the above 1:1 reaction; however, the 1:1 reaction initially produced 1 at $-80\text{ }^\circ\text{C}$, which was then completely converted to 0.5 equiv of 2 at $-50\text{ }^\circ\text{C}$, along with 0.5 equiv of Ph_3CH [CD_2Cl_2 , 300 MHz, $-50\text{ }^\circ\text{C}$: δ 7.27 (t, 6H, *m*-H of *Ph*), 7.20 (t, 3H, *p*-H of *Ph*), 7.10 (d, 6H, *o*-H of *Ph*), 5.55 (s, 1H, *CH*), and 0.5 equiv of the recovered TTPB [CD_2Cl_2 , 300 MHz, $20\text{ }^\circ\text{C}$: δ 8.27 (t, 3H, *p*-H of *Ph*), 7.88 (m, 6H, *m*-H of *Ph*), 7.67 (d, 6H, *o*-H of *Ph*)]. On the other hand, the 2:1 ratio reaction initially gave 1 along with the unreacted ^{Me}SKA at $-80\text{ }^\circ\text{C}$ and then

produced 1 equiv of 2 and Ph_3CH at $-50\text{ }^\circ\text{C}$ with no TTPB left.

1H NMR (CD_2Cl_2 , 300 MHz, $-80\text{ }^\circ\text{C}$) for $[Ph_2C=C(CH=CH)_2CHCMe_2C(OMe)=O\cdots SiMe_3][B(C_6F_5)_4]$ (1). δ 7.34–7.25 (m, 6H, *m*, *p*-H of *Ph*), 7.07 (d, 4H, *o*-H of *Ph*), 6.66 (d, $J = 10.2\text{ Hz}$, 2H, *C(CH=CH)_2CH*), 5.54 (dd, $J = 10.2$ and 3.9 Hz , 2H, *C(CH=CH)_2CH*), 4.21 (s, 1H, *OMe*), 3.53 (t, $J = 3.9\text{ Hz}$, 1H, *C(CH=CH)_2CH*), 1.31 (s, 6H, *CMe_2*), 0.62 (s, 9H, *SiMe_3*). ^{19}F NMR (CD_2Cl_2 , 282 MHz, $-80\text{ }^\circ\text{C}$) for 1: δ -132 (d, $J = 12.7\text{ Hz}$, 8F, *o*-F of C_6F_5), -161 (t, $J = 21.0\text{ Hz}$, 4F, *p*-F of C_6F_5), -165 (m, 8F, *m*-F of C_6F_5).

1H NMR (CD_2Cl_2 , 300 MHz, $-50\text{ }^\circ\text{C}$) for $[Me_3SiOC(OMe)=CMeCH_2CMe_2C(OMe)=O\cdots SiMe_3][B(C_6F_5)_4]$ (2). δ 4.07 (s, 3H, *COOMe*), 3.41 (s, 3H, $=C(OSiMe_3)OMe$), 2.26 (br, 2H, *CH_2*), 1.53 (s, 3H, $=CMe$), 1.28 (s, 6H, *CMe_2*), 0.65 (s, 9H, *SiMe_3*), 0.20 (s, 9H, $=C(OSiMe_3)OMe$). ^{19}F NMR (CD_2Cl_2 , 282 MHz, $-50\text{ }^\circ\text{C}$) for 2: δ -132 (d, $J = 11.3\text{ Hz}$, 8F, *o*-F of C_6F_5), -161 (t, $J = 20.3\text{ Hz}$, 4F, *p*-F of C_6F_5), -165 (m, 8F, *m*-F of C_6F_5).

Attempts to grow single crystals of 2 from a CH_2Cl_2 /hexanes solvent mixture gave oily precipitates. However, laying a hexane solution of 2 equiv of ^{Me}SKA in the presence of a few drops of THF onto a CH_2Cl_2 solution of TTPB in the presence of a few drops of THF at $-30\text{ }^\circ\text{C}$ for 1 week resulted in colorless crystals of $[Me_3Si(THF)]^+[B(C_6F_5)_4]^-$ (3). 1H NMR (CD_2Cl_2 , 300 MHz, $23\text{ }^\circ\text{C}$): δ 4.46 (s, br, 4H, α -*CH*₂, THF), 2.33 (s, br, 4H, β -*CH*₂, THF), 0.66 (s, 9H, Me). ^{19}F NMR (CD_2Cl_2 , 282 MHz, $23\text{ }^\circ\text{C}$): δ -132 (s, br, 8F, *o*-F of C_6F_5), -162 (t, $J = 20.3\text{ Hz}$, 4F, *p*-F of C_6F_5), -166 (s, br, 8F, *m*-F of C_6F_5). Colorless crystals of the ethyl derivative $[Et_3Si(THF)]^+[B(C_6F_5)_4]^-$ (4) were obtained from the reaction of ^{Et}SKA + TTPB in the same manner. 1H NMR (CD_2Cl_2 , 300 MHz, $23\text{ }^\circ\text{C}$): δ 4.51 (s, br, 4H, α -*CH*₂, THF), 2.36 (s, br, 4H, β -*CH*₂, THF), 1.10 (s, br, 15H, Et). ^{19}F NMR (CD_2Cl_2 , 282 MHz, $23\text{ }^\circ\text{C}$): δ -132 (s, br, 8F, *o*-F of C_6F_5), -162 (t, $J = 21.2\text{ Hz}$, 4F, *p*-F of C_6F_5), -166 (s, br, 8F, *m*-F of C_6F_5).

General Polymerization Procedures. Polymerizations were performed either in 30-mL oven-dried glass reactors inside the glovebox or in 25-mL oven- and flame-dried Schlenk flasks interfaced to the dual-manifold Schlenk line. Two different polymerization procedures were employed for comparative studies. In method A procedures, SKA and TTPB were premixed in a 2/1 molar ratio in toluene or CH_2Cl_2 and stirred for 5 min (to generate in situ the active species 2), followed by addition of monomer to start the polymerization. In method B procedures, SKA and monomer were premixed and the polymerization was started by addition of TTPB. For polymerizations using Et_3SiH as the source of the catalyst Et_3Si^+ , the method A procedures involved premixing of Et_3SiH and TTPB in a 1/1 molar ratio in toluene or CH_2Cl_2 and stirring for 10 min to generate in situ the catalyst $Et_3SiB(C_6F_5)_4$,¹³ followed by addition of monomer containing the SKA initiator to start the polymerization. On the other hand, the method B procedures involved premixing of Et_3SiH , SKA, and monomer, followed by addition of TTPB to start the polymerization. After the measured time interval, the polymerization was quenched by addition of 5 mL of 5% HCl-acidified methanol. The quenched mixture was precipitated into 100 mL of methanol, stirred for 1 h, filtered, washed with methanol, and dried in a vacuum oven at $50\text{ }^\circ\text{C}$ overnight to a constant weight.

A Selected Real Polymerization Example. In a argon-filled glovebox, a 30-mL, oven-dried glass reactor was charged with $Ph_3CB(C_6F_5)_4$ (10.8 mg, $11.7\text{ }\mu\text{mol}$) in 10 mL of CH_2Cl_2 . ^{Me}SKA (4.7 μL , $23.4\text{ }\mu\text{mol}$) was added at ambient temperature ($\sim 25\text{ }^\circ\text{C}$). After the resulting mixture was stirred for 5 min, MMA (1.00 mL, 9.35 mmol) was rapidly added to the reactor via a syringe to start the polymerization with a ratio of $[MMA]/[^{Me}SKA]/[Ph_3CB(C_6F_5)_4] = 800:2:1$. The reaction was stirred at ambient temperature for 2 h, after which a 0.2 mL aliquot was withdrawn from the reaction mixture using a syringe and quickly quenched into 1 mL vials containing 0.6 mL of undried "wet" $CDCl_3$ mixed with 250 ppm BHT-H. The reactor was taken out of the box, and the reaction was quenched by addition of 5 mL of 5% HCl-acidified methanol. The quenched mixture was precipitated into 100 mL of methanol, stirred for 1 h, filtered, washed with methanol, and dried in a

Table 1. Results of Methyl Methacrylate (MMA) Polymerization Catalyzed by $\text{Me}_2\text{C}=\text{C}(\text{OMe})\text{OSiMe}_3 + \text{Et}_3\text{SiH} + \text{Ph}_3\text{CB}(\text{C}_6\text{F}_5)_4^a$

run no.	$[\text{Et}_3\text{Si}^+]$ (mol %)	$[\text{M}]_0/[\text{I}]_0$	solvent	$10^4 M_n^b$ (g/mol)	PDI^b (M_w/M_n)	I^*c (%)	$[\text{mm}]^d$ (%)	$[\text{mr}]^d$ (%)	$[\text{rr}]^d$ (%)
1 ^e	0.25	143	toluene	1.88	1.05	76	3.0	33.9	63.1
2 ^f	0.25	143	toluene	2.06	1.05	69	3.0	32.4	64.6
3 ^e	0.25	143	CH_2Cl_2	2.44	1.05	59	2.3	28.7	69.0
4 ^f	0.25	143	CH_2Cl_2	2.15	1.05	67	2.2	28.0	69.8
5 ^f	0.13	143	CH_2Cl_2	1.96	1.04	73	2.3	29.1	68.6

^a Carried out in 10 mL of solvent at room temperature ($\sim 25^\circ\text{C}$) for 1 h with quantitative monomer conversion (by NMR) achieved for all the runs; $[\text{MMA}]_0 = 0.94\text{ M}$; $[\text{Et}_3\text{Si}^+]$ was generated by in situ mixing of Et_3SiH and $\text{Ph}_3\text{CB}(\text{C}_6\text{F}_5)_4$. ^b Number average molecular weight (M_n) and polydispersity index (PDI) determined by gel permeation chromatography relative to PMMA standards in CHCl_3 . ^c Initiator efficiency (I^*) = $M_n(\text{calcd})/M_n(\text{exptl})$, where $M_n(\text{calcd}) = [\text{MW}(\text{MMA})]/([\text{MMA}]_0/[\text{I}]_0)(\text{conversion \%})$. ^d Tacticity determined by ^1H NMR spectroscopy in CDCl_3 (methyl triad distribution: mm , 1.22 ppm; mr , 1.02 ppm; rr , 0.85 ppm¹⁵). ^e Et_3SiH and $\text{Ph}_3\text{CB}(\text{C}_6\text{F}_5)_4$ were premixed and stirred for 10 min followed by addition of MMA containing the initiator SKA. ^f Et_3SiH , $\text{Me}_2\text{C}=\text{C}(\text{OMe})\text{OSiMe}_3$, and MMA were premixed before addition of $\text{Ph}_3\text{CB}(\text{C}_6\text{F}_5)_4$.

vacuum oven at 50°C overnight to a constant weight. The quenched aliquot was analyzed by ^1H NMR to give 100% monomer conversion (see the Polymerization Kinetics section below for details). The isolated and dried polymer was also analyzed by GPC to give $M_n = 1.19 \times 10^5$ g/mol, $\text{PDI} = 1.07$. The dried polymer was also analyzed by ^1H NMR tacticity measurement. ^1H NMR (CDCl_3 , 300 MHz, 23°C) for PMMA: δ 3.60 (s, OMe), 2.05 (d, CH_2), 1.99–1.90 (m, CH_2), 1.82 (s, CH_2), 1.48 (d, CH_2), 1.22 (s, Me, $[\text{mm}] = 2.0\%$), 1.02 (s, Me, $[\text{mr}] = 27.7\%$), 0.85 (s, Me, $[\text{rr}] = 70.3\%$).

Polymerization Kinetics. Kinetic experiments were carried out in a stirred glass reactor at ambient temperature ($\sim 25^\circ\text{C}$) inside the glovebox using stock solutions of the reagents and the procedures described in the literature.¹⁴ Specifically, at appropriate time intervals, 0.2 mL aliquots were withdrawn from the reaction mixture using a syringe and quickly quenched into 1 mL vials containing 0.6 mL of undried “wet” CDCl_3 mixed with 250 ppm BHT–H. The quenched aliquots were analyzed by ^1H NMR. The ratio of $[\text{MMA}]_0$ to $[\text{MMA}]_t$ at a given time t , $[\text{MMA}]_0/[\text{MMA}]_t$, was determined by integration of the peaks for MMA (5.2 and 6.1 ppm for the vinyl signals; 3.4 ppm for the OMe signal) and PMMA (centered at 3.4 ppm for the OMe signals) according to $[\text{MMA}]_0/[\text{MMA}]_t = 2A_{3.4}/3A_{5.2} + 6.1$, where $A_{3.4}$ is the total integral for the peaks centered at 3.4 ppm (typically in the region 3.2–3.6 ppm) and $A_{5.2+6.1}$ is the total integral for both peaks at 5.2 and 6.1 ppm. Apparent rate constants (k_{app}) were extracted from the slopes of the best fit lines to the plots of $[\text{M}]_t/[\text{M}]_0$ vs time.

Polymer Characterizations. Polymer M_n and polydispersity index (M_w/M_n) were measured by gel permeation chromatography (GPC) analyses carried out at 40°C and a flow rate of 1.0 mL/min, with CHCl_3 as the eluent on a Waters University 1500 GPC instrument equipped with one PLgel 5 μm guard and three PLgel 5 μm mixed-C columns (Polymer Laboratories; linear range of molecular weight = 200–2 000 000). The instrument was calibrated with 10 PMMA standards, and chromatograms were processed with Waters Empower software (version 2002). ^1H NMR spectra for the analysis of PMMA and PBMA microstructures were recorded in CDCl_3 and analyzed according to the literature.^{14,15}

Determination of $[\text{M}]/[\text{I}]$ Ratios for Initiator Efficiency (I^*) Calculation of the System by $^{\text{Me}}\text{SKA}/\text{TTPB}$. Because of the unique oxidative activation of $^{\text{Me}}\text{SKA}$ by TTPB (i.e., 1 equiv of TTPB consumes 2 equiv of $^{\text{Me}}\text{SKA}$ to generate 1 equiv of the propagating SKA, vide infra), the actual monomer-to-initiator ratio $[\text{M}]/[\text{I}]$ is not the apparent $[\text{M}]_0/[\text{SKA}]_0$ ratio and is affected by the amount of TTPB used. For a polymerization in an $x[\text{MMA}]_0/y[^{\text{Me}}\text{SKA}]_0/z[\text{TTPB}]_0$ ratio, the total equivalency of the propagating SKA = $y - 2z + z = y - z$, giving a $[\text{M}]/[\text{I}]$ ratio of $x/(y - z)$.

X-ray Crystallographic Analysis of $[\text{Me}_3\text{Si}(\text{THF})]^+[\text{B}(\text{C}_6\text{F}_5)_4]^-$ (3). Single crystals suitable for X-ray diffraction were quickly covered with a layer of Paratone-N oil (Exxon, dried and degassed at $120^\circ\text{C}/10^{-6}$ Torr for 24 h) after the mother liquor was decanted and then mounted on a thin glass fiber and transferred into the cold nitrogen stream of a Bruker SMART CCD diffractometer. The structures were solved by direct methods and refined using the Bruker SHELXTL program library by full-matrix least-squares on F^2 for all reflections.¹⁶ All non-hydrogen atoms were located by difference Fourier synthesis and refined with anisotropic displace-

ment parameters. All hydrogen atoms were included geometrically with U_{iso} tied to the U_{iso} of the parent atoms and refined isotropically. In a unit cell, two independent ion pairs were disclosed.

X-ray crystal structural data for complex **3**: $\text{C}_{31}\text{H}_{17}\text{BF}_{20}\text{OSi}$, $M_r = 824\,035$, $T = 100(2)\text{ K}$, $\lambda = 0.710\,73\text{ \AA}$, crystal dimensions $0.44 \times 0.26 \times 0.07\text{ mm}^3$, triclinic, $P-1$, $a = 10.1347(4)\text{ \AA}$, $b = 17.4222(7)\text{ \AA}$, $c = 19.6456(8)\text{ \AA}$, $\alpha = 67.543(2)^\circ$, $\beta = 80.967(2)^\circ$, $\gamma = 81.909(2)^\circ$, $V = 3153.6(2)\text{ \AA}^3$, $Z = 4$, $\rho_{\text{calcd}} = 1.736\text{ mg/m}^3$, θ range for data collection = $1.99\text{--}31.51^\circ$, 61 876 reflections collected, 19 840 unique ($R_{\text{int}} = 0.0325$), goodness-of-fit on $F^2 = 0.993$, final $R_1 = 0.0423$ and $wR_2 = 0.0953$ with $I > 2\sigma(I)$, residual electron density extremes = 0.440 and -0.392 e \AA^{-3} .

Results and Discussion

MMA Polymerization by $^{\text{Me}}\text{SKA} + \text{Et}_3\text{SiH} + \text{TTPB}$. We initially achieved the controlled MMA polymerization via path c using initiator $^{\text{Me}}\text{SKA}$ and catalyst $[\text{Et}_3\text{Si}(\text{toluene})]^+$ (generated in situ from the reaction of $\text{Et}_3\text{SiH} + \text{TTPB}$ in toluene¹³), affording PMMA with $\text{PDI} = 1.05$, initiator efficiencies (I^*) in the range of 59–76%, and syndiotacticity $[\text{rr}] = 64\%$ (toluene) or 69% (CH_2Cl_2), Table 1. Premixing of Et_3SiH and TTPB is not required, and TTPB can be added last for achieving similar polymerization results. Control runs using each of these three reagents alone or combinations of two reagent pairs ($\text{Et}_3\text{SiH}/\text{TTPB}$ or $\text{Et}_3\text{SiH}/^{\text{Me}}\text{SKA}$ pairs) showed no polymerization activity.

Polymerization of MMA by $^{\text{Me}}\text{SKA} + \text{TTPB}$. Surprising results were revealed when we carried out a control of the last possible combination using the $^{\text{Me}}\text{SKA}/\text{TTPB}$ pair (no Et_3SiH): it is highly active for controlled methacrylate polymerization! Thus, addition of 1 equiv of TTPB to a CH_2Cl_2 solution containing 400 equiv of MMA and 2 equiv of $^{\text{Me}}\text{SKA}$ achieved 97% MMA conversion in 20 min at 25°C , affording PMMA with $M_n = 3.87 \times 10^4$, $\text{PDI} = 1.10$, and $[\text{rr}] = 69\%$. The measured M_n value (against PMMA standards) is double what is calculated based on the apparent $[\text{MMA}]/[^{\text{Me}}\text{SKA}]$ ratio of 200; however, the unique activation mechanism of this system (vide infra) gives the actual monomer-to-initiator ratio $[\text{M}]/[\text{I}]$ of 400 (see Experimental Section), for a quantitative initiator efficiency. Under the same conditions, quantitative BMA conversion was achieved in 60 min, yielding PBMA of $M_n = 5.44 \times 10^4$, $\text{PDI} = 1.06$, $[\text{rr}] = 80\%$, and again a quantitative initiator efficiency. High M_n (1.86×10^5) PMMA was readily obtained using a $[\text{M}]/[\text{I}]$ ratio of 1600.

The initial kinetic profiling of the MMA polymerization was performed at a $[\text{M}]/[\text{I}]$ ratio of 800 at 25°C in CH_2Cl_2 . In the first approach, 2 equiv of $^{\text{Me}}\text{SKA}$ and 1 equiv of TTPB were premixed and stirred for 5 min, followed by addition of 800 equiv of MMA to start the polymerization (method A). A plot of the PMMA M_n ((2.05×10^3) to (1.19×10^5)) vs MMA conversion (2.1% to 100%) gave a linear relationship ($R^2 =$

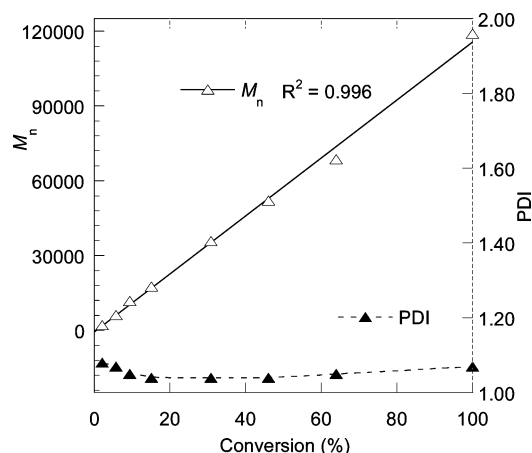


Figure 1. Plots of the poly(methyl methacrylate) number-average molecular weight (M_n) and polydispersity index (PDI) vs methyl methacrylate (MMA) conversion. Conditions: 25 °C, 10 mL of CH_2Cl_2 , [monomer]/[initiator] = 800, method A (2 equiv of $\text{Me}_2\text{C}=\text{C}(\text{OMe})\text{OSiMe}_3$ and 1 equiv of $\text{Ph}_3\text{CB}(\text{C}_6\text{F}_5)_4$ were premixed and stirred for 5 min, followed by addition of 800 equiv of MMA to start the polymerization).

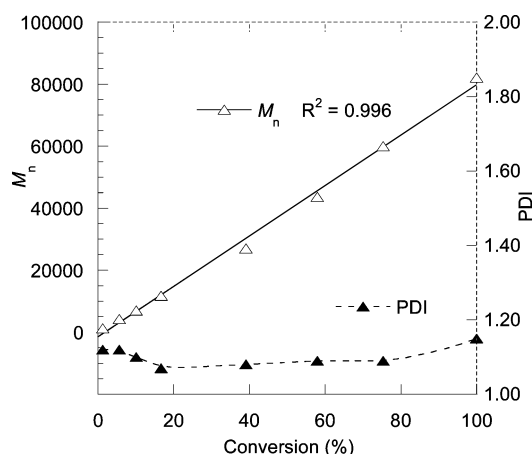


Figure 2. Plots of the poly(methyl methacrylate) number-average molecular weight (M_n) and polydispersity index (PDI) vs methyl methacrylate (MMA) conversion. Conditions: 25 °C, 10 mL of CH_2Cl_2 , [monomer]/[initiator] = 800, method B (800 equiv of MMA and 2 equiv of $\text{Me}_2\text{C}=\text{C}(\text{OMe})\text{OSiMe}_3$ were premixed before addition of 1 equiv of $\text{Ph}_3\text{CB}(\text{C}_6\text{F}_5)_4$).

0.996), whereas the molecular weight distribution (MWD) remains narrow for all conversions (PDI = 1.04–1.08), Figure 1. The I^* values range from 64% to 82%, and the final isolated polymer has a $[rr]$ value of 70%.

In the second approach, 800 equiv of MMA and 2 equiv of MeSKA were premixed before addition of 1 equiv of TTPB to start the polymerization (method B). The overall characteristics of the polymerization by method B are similar to those observed by method A, except for slightly higher PDI values and essentially quantitative I^* values for method B (Figure 2). This comparative study implies that the active species generated from $\text{MeSKA} + \text{TTPB}$ is somewhat unstable in the absence of monomer or polymer.

We subsequently examined solvent and SKA structure effects on polymerization. Methacrylate polymerizations in toluene are similarly active and controlled. Using method A in a $[\text{M}]/[\text{I}]$ ratio of 400 at 25 °C, quantitative monomer conversion was achieved in <40 min (MMA) or <60 min (BMA), affording the corresponding polymer with PDI = 1.04 (for both polymers) and $I^* = 75\%$ and 92%, respectively. Donor solvents such as THF shut down the polymerization, in contrast to the nucleophile-catalyzed GTP which routinely employs THF as a solvent. Replacing MeSKA with EtSKA resulted in lower polymerization activity.

Oxidative Activation of MeSKA by TTPB Leading to Active Species. To probe the structure of the active species derived from the activation of SKA with TTPB, we first examined 1:1 and 2:1 ratio reactions of $\text{MeSKA} + \text{TTPB}$ in CD_2Cl_2 at room temperature, which yielded an orange-yellow solution and a colorless solution, respectively. However, both reactions produced identical species **C** ($\text{R} = \text{Me}$, Scheme 1) and Ph_3CH as the main products; there was still 0.5 equiv of TTPB left in the 1:1 reaction, accounting for its observed color, and both reactions showed complex NMR features due to the presence of other species. To determine if the other species present were derived from the reaction itself or decomposition of **C**, we carried out variable temperature NMR studies of both ratio reactions. For the 1:1 reaction at -80 °C, *electrophilic addition* of Ph_3C^+ , via the para-carbon of Ph, to MeSKA cleanly forms the addition product **1** (Scheme 2); the unactivated form of **1** (i.e., without the $\text{Me}_3\text{SiB}(\text{C}_6\text{F}_5)_4$ moiety attached) was previously generated from the reaction of $\text{MeSKA} + \text{Ph}_3\text{CClO}_4$ at 25 °C.¹⁷ However, in startling contrast to its unactivated form, **1** begins to convert to **2** at -70 °C, with concomitant formation of Ph_3CH , and is completely transformed to **2** (0.5 equiv) at -50 °C, plus 0.5 equiv of Ph_3CH and 0.5 equiv of the released TTPB (Figure 3).

Formation of **2** can be explained by Michael addition of MeSKA to the Me_3Si^+ -activated MMA generated by vinylogous *hydride abstraction* of MeSKA with Ph_3C^+ (Scheme 2), given that **1** reversibly releases MeSKA and TTPB above -70 °C. Such

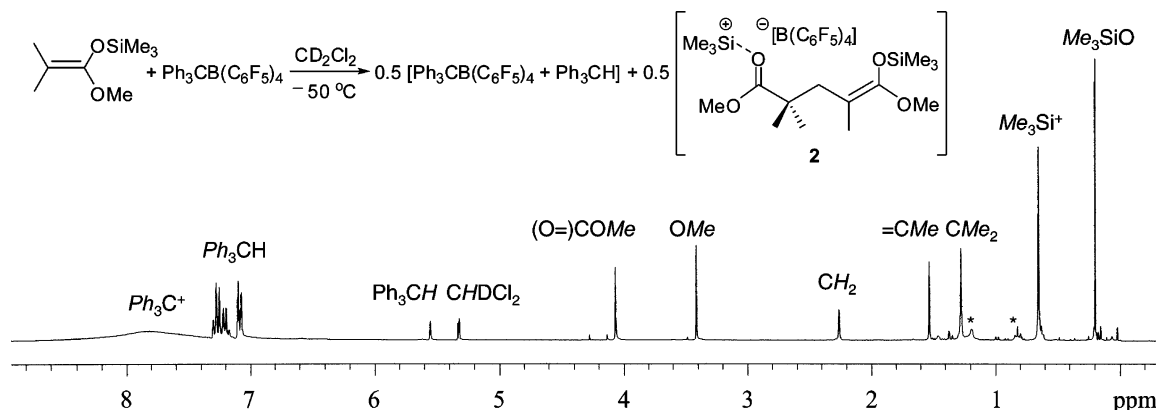


Figure 3. ^1H NMR spectrum for in situ generation of **2** from the 1:1 ratio reaction of $\text{Me}_2\text{C}=\text{C}(\text{OMe})\text{OSiMe}_3$ and $\text{Ph}_3\text{CB}(\text{C}_6\text{F}_5)_4$ at -50 °C in CD_2Cl_2 ; this spectrum also contains a small amount of hexanes (peaks marked with an *) brought forward from the starting reagents, and the unlabeled small peaks are attributed to the other isomer and minor impurities due to decomposition of **2**. The 2:1 reaction gives the same product with all the 1 equiv of $\text{Ph}_3\text{CB}(\text{C}_6\text{F}_5)_4$ added being consumed.

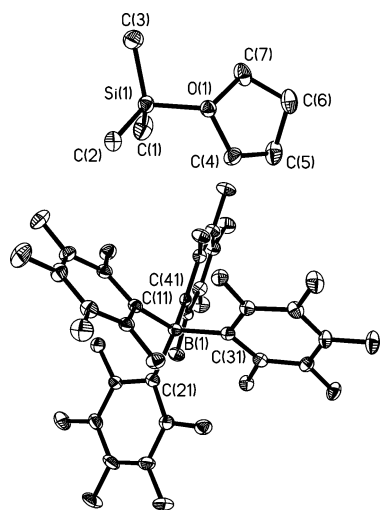


Figure 4. X-ray crystal structure of $[\text{Me}_3\text{Si}(\text{THF})]^+[\text{B}(\text{C}_6\text{F}_5)_4]^-$ (**3**) with thermal ellipsoids drawn at the 50% probability level. Selected bond lengths [Å] and angles [deg]: Si–O 1.784(1), Si–C(1) 1.841(2), Si–C(2) 1.843(2), Si–C(3) 1.836(2), B–C(11) 1.657(2), B–C(21) 1.659(2), B–C(31) 1.654(2), B–C(41) 1.657(2); C(1)–Si–C(2) 113.53(10), C(1)–Si–C(3) 114.04(10), C(2)–Si–C(3) 114.09(9), O–Si–C(1) 105.56(8), O–Si–C(2) 104.56(7), O–Si–C(3) 103.61(7).

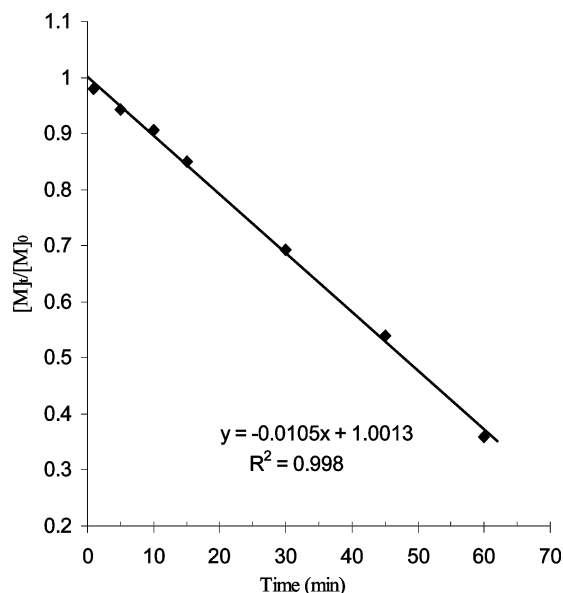


Figure 5. Zero-order plot of $[\text{M}]/[\text{M}]_0$ vs time for the methyl methacrylate (MMA) polymerization by the $\text{Me}_2\text{C}=\text{C}(\text{OMe})\text{OSiMe}_3$ ($^{\text{Me}}\text{SKA}$) + $\text{Ph}_3\text{CB}(\text{C}_6\text{F}_5)_4$ (TTPB) system in CH_2Cl_2 at 25 °C using method A in a $\text{MMA}/^{\text{Me}}\text{SKA}/\text{TTPB}$ ratio = 800/2/1: $[\text{MMA}]_0 = 0.935$ M, $[\text{MeSKA}]_0 = 2.34$ mM, $[\text{TTPB}]_0 = 1.17$ mM.

H^- abstraction was observed in the silyl enol ether + Ph_3CBF_4 reaction leading to α,β -unsaturated ketones and also in the zirconocene *tert*-butyl enolate + TTPB reaction leading to the formation of a zirconocene-carboxylate dication after subsequent elimination of methane and isobutene.¹⁸ Likewise, the 2:1 ratio reaction showed initial formation of **1** (plus the unreacted $^{\text{Me}}\text{SKA}$) at -80 °C, followed by generation of 1 equiv of **2** and Ph_3CH at -50 °C (no TTPB left). Unlike its unactivated form,¹⁹ **2** is somewhat unstable and starts decomposition to some extent at $T \geq -40$ °C, which explains why the polymerization with method B (in situ generation of **2** in the presence of monomer) always gives higher I^* values than those by method A (pregeneration of **2** before addition of MMA).

Structure of Active Species Involved in the $^{\text{Me}}\text{SKA}$ + TTPB System. Attempts to obtain single crystals of **2** for

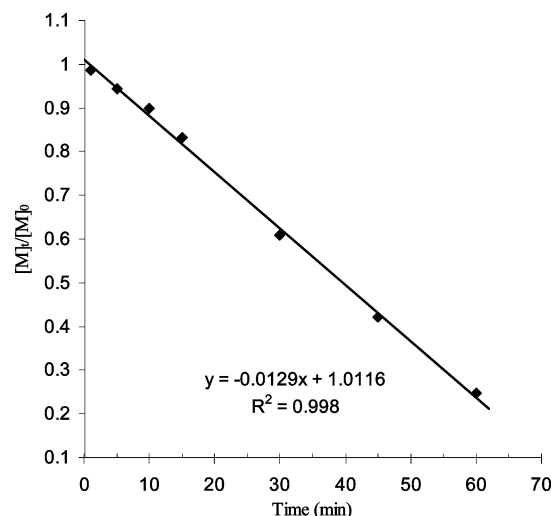
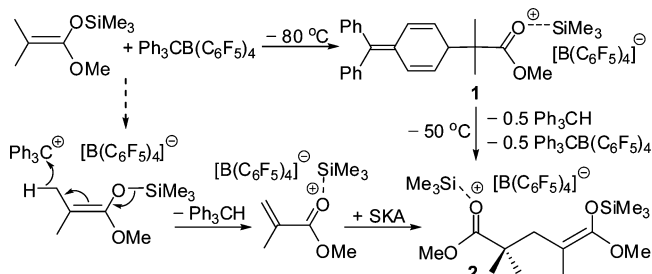


Figure 6. Zero-order plot of $[\text{M}]/[\text{M}]_0$ vs time for the methyl methacrylate (MMA) polymerization by the $\text{Me}_2\text{C}=\text{C}(\text{OMe})\text{OSiMe}_3$ ($^{\text{Me}}\text{SKA}$) + $\text{Ph}_3\text{CB}(\text{C}_6\text{F}_5)_4$ (TTPB) system in CH_2Cl_2 at 25 °C using method B in a $\text{MMA}/^{\text{Me}}\text{SKA}/\text{TTPB}$ ratio = 800/2/1: $[\text{MMA}]_0 = 0.935$ M, $[\text{MeSKA}]_0 = 2.34$ mM, $[\text{TTPB}]_0 = 1.17$ mM.

Scheme 2. Oxidative Activation of $\text{Me}_2\text{C}=\text{C}(\text{OMe})\text{OSiMe}_3$ by $\text{Ph}_3\text{CB}(\text{C}_6\text{F}_5)_4$: Initiation Step



possible structural characterizations yielded oily precipitates and were also plagued by its thermal instability at $T \geq -40$ °C. However, single crystals of its silyloxonium analogue, trimethylsilylated tetrahydrofuran (THF) oxonium salt $[\text{Me}_3\text{Si}(\text{THF})]^+[\text{B}(\text{C}_6\text{F}_5)_4]^-$ (**3**), were obtained by slow mixing of a hexane solution of $^{\text{Me}}\text{SKA}$ and a CH_2Cl_2 solution of TTPB in the presence of a small amount of THF at -30 °C. Although **3** was previously generated in situ from the reaction of Me_3SiH + TTPB + THF in CD_2Cl_2 at -78 °C and reported to be only stable below -20 °C,²⁰ this in situ low-temperature crystallization technique allowed for growing single crystals and subsequent structural characterization of **3** by X-ray diffraction analysis. The solid-state structure of **3** consists of two independent ion pairs in a unit cell with similar metric parameters, only one of which is shown in Figure 4 and briefly discussed here. The four-coordinate Si center adopts a distorted tetrahedral geometry with the sum of the C–Si–C angles being 341.7°, and the Si atom sits above the Me_3 -basal plane by 0.463 Å. The average C–Si–C angle of 114° in **3** compares to 113°, 114°, 115°, 117°, and 118° observed in $[\text{Me}_3\text{Si}(\text{py})]^+\text{I}^-$,²¹ $[\text{Et}_3\text{Si}(\text{toluene})]^+[\text{B}(\text{C}_6\text{F}_5)_4]^-$,¹³ $[\text{Pr}_3\text{Si}(\text{MeCN})]^+[\text{Br}_3\text{CB}_9\text{H}_5]^-$,²² $^{\text{Pr}}\text{Pr}_3\text{Si}(\text{Br}_6\text{CB}_{11}\text{H}_6)$,²³ and $[\text{Me}_3\text{Si}][\text{C}_2\text{H}_5\text{CB}_{11}\text{H}_{11}]$,²⁴ respectively. The three Si–C bonds in **3** have an essentially identical bond length [1.840 (av) Å], so do the four B–C bonds [1.657 (av) Å]. The Si–O bond length of 1.784(1) Å is shorter than the calculated value of 1.842 Å²⁰ by ~ 0.06 Å but slightly longer than that observed in $\text{Ph}_3\text{SiOCIO}_3$ [1.744(4) Å].²⁵ Overall, the structural analysis of **3** that simulates that of **2** confirms the formation of the silyloxonium borate salt consisting of the

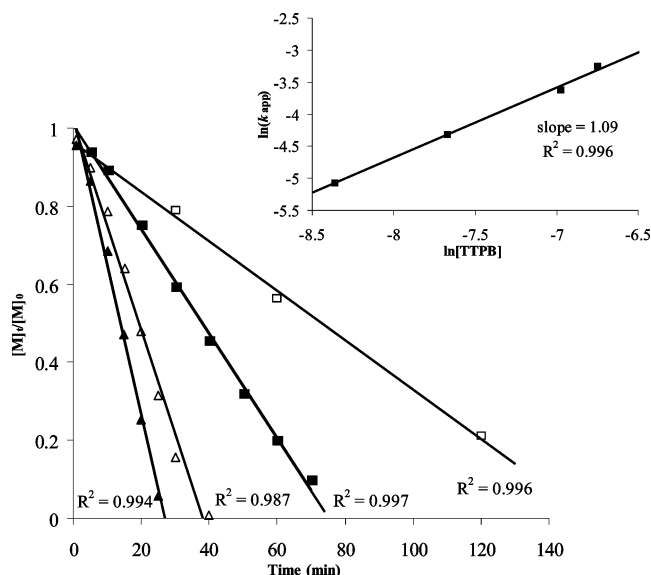


Figure 7. Zero-order kinetic plots for the methyl methacrylate (MMA) polymerization by the $\text{Me}_2\text{C}=\text{C}(\text{OMe})\text{OSiMe}_3$ (MeSKA) + $\text{Ph}_3\text{CB}(\text{C}_6\text{F}_5)_4$ (TTPB) system in CH_2Cl_2 at 25 °C: $[\text{MMA}]_0 = 0.935 \text{ M}$; $[\text{MeSKA}]_0 = 4.67 \text{ mM}$; $[\text{TTPB}]_0 = 1.17 \text{ mM}$ (▲), 0.934 mM (△), 0.467 mM (■), 0.234 mM (□). Inset: plot of $\ln(k_{\text{app}})$ vs $\ln[\text{TTPB}]_0$.

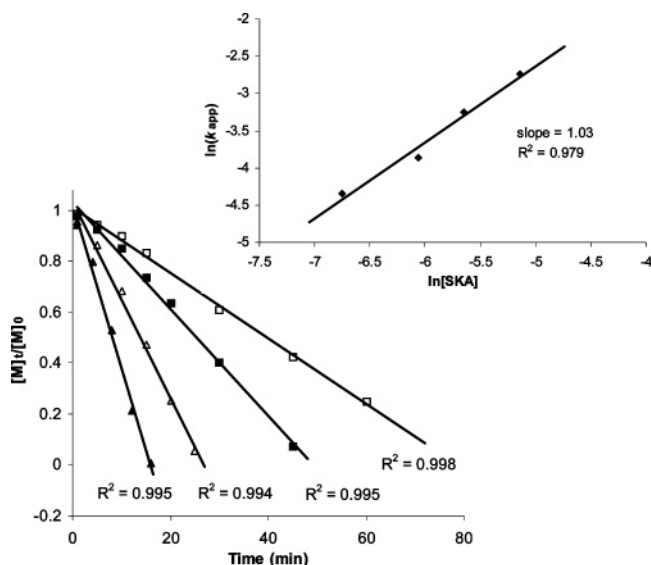


Figure 8. Zero-order kinetic plots for the methyl methacrylate (MMA) polymerization by the $\text{Me}_2\text{C}=\text{C}(\text{OMe})\text{OSiMe}_3$ (MeSKA) + $\text{Ph}_3\text{CB}(\text{C}_6\text{F}_5)_4$ (TTPB) system in CH_2Cl_2 at 25 °C: $[\text{MMA}]_0 = 0.935 \text{ M}$; $[\text{TTPB}]_0 = 1.17 \text{ mM}$; $[\text{MeSKA}]_0 = 7.02 \text{ mM}$ (▲), 4.68 mM (△), 3.51 mM (■), 2.34 mM (□). Inset: plot of $\ln(k_{\text{app}})$ vs $\ln[\text{SKA}]$ where $[\text{SKA}] = [\text{MeSKA}]_0 - [\text{TTPB}]_0$.

trimethylsilylated oxonium cation and the unassociated borate anion.

Kinetics and Mechanism of MMA Polymerization by MeSKA + TTPB. The uncovering of the activation/initiation pathway of this system has led to further elucidation of its propagation mechanism with the aid of kinetics studies. The polymerization follows zero-order kinetics in monomer concentration $[\text{M}]$, regardless of the $\text{MMA}/\text{MeSKA}/\text{TTPB}$ ratio and the method, although the observed rate by method B is ~ 1.2 times of that by method A (Figure 5 vs Figure 6). These results indicate that method B is desirable for propagation kinetic studies due to its quantitative or near quantitative initiator efficiency and rapid, instantaneous generation of the active propagating species.

Scheme 3. Proposed Bimolecular, Activated-Monomer Propagation Mechanism

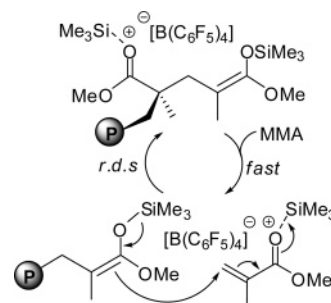


Figure 7 summarizes the kinetics of the polymerizations by $400\text{MMA}/2\text{MeSKA}/x\text{TTPB}$ ($x = 0.5, 0.4, 0.2$, and 0.1) at 25 °C. There is no induction period observed and the zero-order in $[\text{M}]$ kinetics holds true for all the ratios used. The polymerization is first order with respect to the catalyst $[\text{Me}_3\text{Si}^+]$ concentration, given by the slope = 1.09(8) from double logarithm plots of k_{app} as a function of $[\text{TTPB}]$, thereby establishing activated monomer polymerization.

The polymerization is also first order in the propagating $[\text{SKA}]$, given by the slope = 1.03 from a plot of $\ln(k_{\text{app}})$ vs $\ln[\text{SKA}]$ (Figure 8). Overall, these findings are consistent with the propagation mechanism depicted in Scheme 3 in which the C–C bond formation via *intermolecular* Michael addition of the polymeric SKA to the silyl cation-activated MMA is the rate-determining step (rds), and the release of the catalyst from the ester group of the growing polymer chain to the incoming MMA is relatively fast.

Conclusions

In summary, by a combined study of polymerization, structure, and kinetics, we have developed the new polymerization system based on oxidative activation of the GTP initiator SKA with a catalytic amount of the ubiquitous olefin polymerization activator $\text{Ph}_3\text{CB}(\text{C}_6\text{F}_5)_4$. Remarkably, species **2** derived from the oxidative activation of SKA is the first MMA addition product of the polymerization, the highly active propagating species structure containing both nucleophilic (SKA, which attacks the activated monomer) and electrophilic (Me_3Si^+ , which activates the incoming monomer) catalyst sites, thereby promoting controlled polymerization via cooperative catalysis. In addition to its mechanistic distinction in initiation and propagation, this metal-free system readily produces PMMA of low to high M_n ($> 10^5$) with a narrow MWD (1.04–1.12) at ambient temperature.

Acknowledgment. This work was supported by the donors of the Petroleum Research Fund, administered by the American Chemical Society. We thank Logan Garner for some initial studies, Susie Miller for X-ray data collection, Dr. Hongping Zhu for crystal structure solution, Prof. Tom Rovis for discussions, and Boulder Scientific Co. for the gift of $\text{Ph}_3\text{CB}(\text{C}_6\text{F}_5)_4$.

Supporting Information Available: Crystallographic data for **3** (CIF). This material is available free of charge via the Internet at <http://pubs.acs.org>.

References and Notes

- (1) (a) Sogah, D. Y.; Hertler, W. R.; Webster, O. W.; Cohen, G. M. *Macromolecules* **1987**, *20*, 1473–1488. (b) Hertler, W. R.; Sogah, D. Y.; Webster, O. W.; Trost, B. M. *Macromolecules* **1984**, *17*, 1417–1419. (c) Webster, O. W.; Hertler, W. R.; Sogah, D. Y.; Farnham, W. B.; RajanBabu, T. V. *J. Am. Chem. Soc.* **1983**, *105*, 5706–5708.

- (2) Webster, O. W. *Adv. Polym. Sci.* **2004**, *167*, 1–34.
- (3) (a) Müller, A. H. E.; Litvinenko, G.; Yan, D. *Macromolecules* **1996**, *29*, 2346–2353. (b) Quirk, R. P.; Kim, J.-S. *J. Phys. Org. Chem.* **1995**, *8*, 242–248. (c) Quirk, R. P.; Bidinger, G. P. *Polym. Bull.* **1989**, *22*, 63–70.
- (4) (a) Rodriguez-Delgado, A.; Chen, E. Y.-X. *J. Am. Chem. Soc.* **2005**, *127*, 961–974. (b) Bolig, A. D.; Chen, E. Y.-X. *J. Am. Chem. Soc.* **2001**, *123*, 7943–7944.
- (5) (a) Stojcevic, G.; Kim, H.; Taylor, N. J.; Marder, T. B.; Collins, S. *Angew. Chem., Int. Ed.* **2004**, *43*, 5523–5526. (b) Li, Y.; Ward, D. G.; Reddy, S. S.; Collins, S. *Macromolecules* **1997**, *30*, 1875–1883.
- (6) (a) Kobayashi, S.; Murakami, M.; Mukaiyama, T. *Chem. Lett.* **1985**, *14*, 1535–1538. (b) Kobayashi, S.; Murakami, M.; Mukaiyama, T. *Chem. Lett.* **1985**, *14*, 953–956. (c) Mukaiyama, T.; Kobayashi, S.; Murakami, M. *Chem. Lett.* **1985**, *14*, 447–450. (d) Mukaiyama, T.; Kobayashi, S.; Murakami, M. *Chem. Lett.* **1984**, *13*, 1759–1762.
- (7) (a) Bochmann, M.; Lancaster, S. J. *J. Organomet. Chem.* **1992**, *434*, C1–C5. (b) Chien, J. C. W.; Tsai, W.-M.; Rausch, M. D. *J. Am. Chem. Soc.* **1991**, *113*, 8570–8571.
- (8) Chen, E. Y.-X.; Marks, T. J. *Chem. Rev.* **2000**, *100*, 1391–1434.
- (9) (a) Noyori, R.; Murata, S.; Suzuki, M. *Tetrahedron* **1981**, *37*, 3899–3910. (b) Murata, S.; Suzuki, M.; Noyori, R. *J. Am. Chem. Soc.* **1980**, *102*, 3248–3249.
- (10) Ute, K.; Ohnuma, H.; Kitayama, T. *Polym. J.* **2000**, *32*, 1060–1062.
- (11) Allen, R. D.; Long, T. E.; McGrath, J. E. *Polym. Bull.* **1986**, *15*, 127–134.
- (12) (a) Hasegawa, A.; Naganawa, Y.; Fushimi, M.; Ishihara, K.; Yamamoto, H. *Org. Lett.* **2006**, *8*, 3175–3178. (b) See ref 1(a). (c) RajanBabu, T. V. *J. Org. Chem.* **1984**, *49*, 2083–2089.
- (13) Lambert, J. B.; Zhang, S.; Stern, C. L.; Huffman, J. C. *Science* **1993**, *260*, 1917–1918.
- (14) (a) See ref. 4(a). (b) Rodriguez-Delgado, A.; Mariott, W. R.; Chen, E. Y.-X. *Macromolecules* **2004**, *37*, 3092–3100.
- (15) (a) Bovey, F. A.; Mirau, P. A. *NMR of Polymers*; Academic Press: San Diego, CA, 1996. (b) Chujo, R.; Hatada, K.; Kitamaru, R.; Kitayama, T.; Sato, H.; Tanaka, Y. *Polym. J.* **1987**, *19*, 413–424. (c) Ferguson, R. C.; Ovenall, D. W. *Polym. Prepr.* **1985**, *26*, 182–183. (d) Subramanian, R.; Allen, R. D.; McGrath, J. E.; Ward, T. C. *Polym. Prepr.* **1985**, *26*, 238–240.
- (16) *SHELXTL*, version 6.12; Bruker Analytical X-ray Solutions: Madison, WI, 2001.
- (17) Fukuzumi, S.; Ohkubo, K.; Otera, J. *J. Org. Chem.* **2001**, *66*, 1450–1454.
- (18) (a) Jung, M. E.; Pan, Y.-G.; Rathke, M. W.; Sullivan, D. F.; Woodbury, R. P. *J. Org. Chem.* **1977**, *42*, 3961–3963. (b) Lian, B.; Toupet, L.; Carpentier, J.-F. *Chem. Eur. J.* **2004**, *10*, 4301–4307.
- (19) Brittain, W. J. *Am. Chem. Soc.* **1988**, *110*, 7440–7444.
- (20) Olah, G. A.; Wang, Q.; Li, X.-Y.; Rasul, G.; Prakash, G. K. S. *Macromolecules* **1996**, *29*, 1857–1861.
- (21) Hensen, K.; Zengerly, T.; Pickel, P.; Klebe, G. *Angew. Chem., Int. Ed. Engl.* **1983**, *22*, 725–726.
- (22) Xie, Z.; Liston, D. J.; Jelinek, T.; Mitro, V.; Bau, R.; Reed, C. A. *J. Chem. Soc., Chem. Commun.* **1993**, 384–386.
- (23) Reed, C. A.; Xie, Z.; Bau, R.; Benesi, A. *Science* **1993**, *262*, 402–404.
- (24) Küppers, T.; Bernhardt, E.; Eujen, R.; Willner, H.; Lehmann, C. W. *Angew. Chem., Int. Ed.* **2007**, *46*, 6346–6349.
- (25) Prakash, G. K. S.; Keyaniyan, S.; Aniszfild, R.; Heiliger, L.; Olah, G. A.; Stevens, R. C.; Choi, H.-K.; Bau, R. *J. Am. Chem. Soc.* **1987**, *109*, 5123–5126.

MA702015W